Structural characterization and properties of the perovskite (NaLa)(MW)O_6 (M = Co, Ni): two new members in the group–subgroup relations for the perovskite-type structures

M. Angeles Arillo, Julio Gómez, María L. López, Carlos Pico and M. Luisa Veiga

Departamento de Química Inorgánica I, Facultad de Ciencias Químicas, Universidad Complutense, Ciudad Universitaria, E-28040 Madrid, Spain

The crystal structures of (NaLa)(MW)O_6 (M = Co, Ni) suggest that both adopt a monoclinic perovskite-type structure [M = Co: $a = 5.546(3)$, $b = 5.545(4)$, $c = 7.903(6)$ Å, $\beta = 89.99(3)^\circ$; M = Ni: $a = 5.517(5)$, $b = 5.518(7)$, $c = 7.862(2)$ Å, $\beta = 90.02(4)^\circ$; space group $P2_1/m$]. The structure consists of an ordered arrangement of MO_6 and WO_6 octahedra (in B sites) which share corners and alternate planes of La and Na cations along the *c*-axis (in A sites). This structure is analysed on the basis of a general group–subgroup symmetry relationship for some perovskites that were previously described, and the electronic and magnetic properties of both compounds are discussed.

Mixed oxides ABO_3 with the cubic perovskite structure show octahedral coordination for B atoms and cuboctahedral coordination for A atoms, and the parent structure is described in the space group $Pm3m$ (or $P4/m\ 32/m$ in its complete form). In the cubic unit cell, atom A is located on the Wyckoff position 1b (site symmetry $m3m$) with coordinates (1/2, 1/2, 1/2), atom B on the 1a position (site symmetry $m3m$) with coordinates (0, 0, 0), and oxygen atoms occupy the 3d positions (site symmetry $4/mm.m$, coordinates (1/2, 0, 0; 0, 1/2, 0; 0, 0, 1/2).

The perovskite crystal structure can be described in several ways:[1–3] (1) by stating its space group and the equivalent positions that are occupied; (2) starting from the BO_6 octahedra sharing corners with other similar polyhedra; this scheme allows B—O—B and O—B—O bond angles of 180° and 90° respectively. The centres of eight octahedra define a cube which corresponds to the parent unit cell, as is depicted in Fig. 1. There is a rather large cuboctahedral cavity in the centre of the unit cell that is occupied by A cations; (3) considering cubic close-packing of A and oxygen atoms, in the stoichiometric ratio 1 : 3, in which a 1/4 of the octahedral holes are occupied by B cations in an ordered fashion.

More detailed studies on perovskite-type structures have been carried out by Glazer[4] for the ABX_3 derivatives, based on BX_6 tilting and the possible space groups derived from the structural characteristics. Anderson *et al.*[5] reported a survey of A′A″B′B″O_6 double perovskites, discussing the factors that influence B cation arrangement in several compounds, but this study was limited to the ordering in the B sublattice. In this sense, Sekiya *et al.*[6] proposed a new kind of ordering in the A sublattice on the basis of X-ray diffraction and IR spectra. Such assumptions were confirmed by neutron diffraction data for the isomorphic phase (NaLa)(MgTe)O_6.[7]

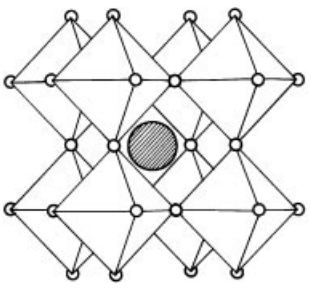

Fig. 1 Ideal perovskite structure

A large number of mixed oxides with a common perovskite-type structure have so far been reported, in which there are deviations from the ideal stoichiometry, various A and/or B cations, and which very frequently belonging to non-cubic space groups. Bearing in mind our previous studies in this context, this paper reports the structural characterization and some physical properties of two isomorphic phases, (NaLa)(MW)O_6 (M = Co, Ni); both structures are discussed and a broad description of the symmetry group–subgroup relationship in the perovskite field is also shown.

Experimental

Polycrystalline samples (NaLa)(MW)O_6 were prepared by sol–gel techniques from powdered mixtures of WO_3, $NaNO_3$, $La(NO_3)_3{\cdot}6H_2O$ and $M(NO_3)_2{\cdot}6H_2O$ (M = Ni, Co) (all reagents supplied by Merck, Germany) in stoichiometric ratio. Each mixture was preheated in an aluminia crucible at 498 K for 24 h, and 773 K for 72 h. Finally, the samples were heated in air at 1173 K for 1 day.

X-Ray diffraction patterns were recorded with a Philips X'Pert-MPD diffractometer and a 3051/100 goniometer, using Ni-filtered Cu-Kα radiation. A 2θ step size of 0.04° was used. The Rietveld profile analysis method[8] was employed for refinement of the X-ray diffraction results in the perovskites (NaLa)(MW)O_6. The X-ray diffraction patterns were analysed using the Rietveld method,[4] using the program Fullprof.[9]

The magnetic susceptibility measurements were carried out using a DSM8 pendulum susceptometer based on the Faraday method. The maximum applied magnetic field was 15 kG with $H(dH/dz) = 29\ kG^2\ cm^{-1}$. The equipment was calibrated with $Hg[Co(SCN)_4]$ and $Gd_2(SO_4)_3{\cdot}8H_2O$, which have χ independent of the field in the temperature range of the measurements. The magnetic susceptibility data were corrected taking into account the ionic diamagnetic contribution.[10]

Results and Discussion

Structural characterization

Structural characterization of the title compounds, (NaLa)(MW)O_6, was carried out by means of X-ray diffraction. The powder patterns were characteristic of a perovskite-type structure. The expected reflections were split, corresponding to a noticeable distortion from the ideal cubic symmetry. All the reflections could be satisfactorily indexed on the basis

of a monoclinic unit cell, space group $P2_1/m$, with the parameters $a \approx b \approx a_o\sqrt{2}$, $c \approx 2a_o$ (where a_o is the unit cell parameter of the ideal perovskite), and β is close to 90°. Structural data obtained from the Rietveld refinement are reported in Table 1 and the R factors indicate a reliable structural model. Atomic coordinates are given in Tables 2 (M = Co) and 3 (M = Ni). The model provides a good agreement between observed and calculated X-ray diffraction profiles as shown in Fig. 2. From these data the most representative bond lengths are obtained and they are gathered in Tables 4 (Co) and 5 (Ni) as well as the comparison with the sums of Shannon ionic radii for each case. The above results indicate that the MO_6 and WO_6 octahedra are very distorted, although the mean bond distances are similar to the Shannon ones, and the Na and La polyhedra are defined by ten oxygen atoms in both compounds as a result of the structure distortion.

Fig. 3 shows a structural model for $(NaLa)(MW)O_6$, in which each WO_6 octahedron shares all its corners with other MO_6 units in an ordered two-dimensional arrangement and *vice versa* (depicted by shaded and white polyhedra). Na and La cations are intercalated between such planes of octahedra in an alternating manner, along the c axis. However, the best refinement is obtained when some degree of disorder is taken into account for the distribution of A cations in both phases; final results correspond to 5.6% (for Co oxide) and 6.6% (Ni oxide).

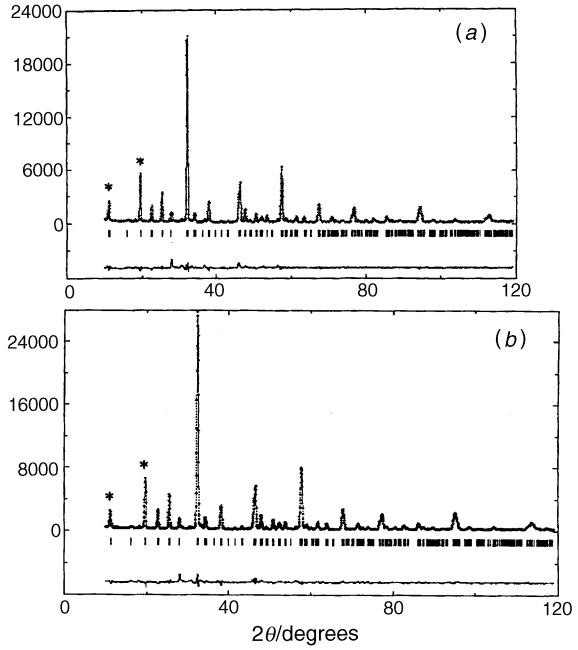

Fig. 2 Observed (···), calculated (—) and difference profiles for $(NaLa)(WM)O_6$: (*a*) M = Co, (*b*) M = Ni

Table 1 Crystallographic data for $NaLaMWO_6$ (M = Ni and Co)

	$NaLaCoWO_6$	$NaLaNiWO_6$
a/Å	5.546(3)	5.517(5)
b/Å	5.545(4)	5.517(7)
c/Å	7.903(6)	7.862(2)
β/degrees	89.99(3)	90.02(4)
V/Å^3	243.04	239.33
Z	2	2
R_p (%)	13.6	11.3
R_{wp} (%)	18.5	15.2
R_e (%)	6.06	5.24
R_B (%)	6.84	5.96

Table 2 Fractional atomic coordinates of $NaLaCoWO_6$

atom	position	x	y	z	occupation
La(1)[a]	2e	0.260(1)	0.250	0.004(3)	0.06
La(2)[a]	2e	0.226(7)	0.250	0.507(7)	0.94
Na(1)[a]	2e	0.226(7)	0.250	0.507(7)	0.06
Na(2)[a]	2e	0.260(1)	0.250	0.004(3)	0.94
Co	2e	0.758(6)	0.250	0.254(7)	1.00
W	2e	0.745(1)	0.250	0.731(3)	1.00
O(1)	4f	0.465(1)	0.434(7)	0.712(8)	1.00
O(2)	4f	0.024(8)	0.041(0)	0.216(5)	1.00
O(3)	2e	0.681(1)	0.250	0.523(2)	1.00
O(4)	2e	0.732(5)	0.250	0.011(3)	1.00

[a]Disordered in A-plane: 5.6%.

Table 3 Fractional atomic coordinates of $NaLaNiWO_6$

atom	position	x	y	z	occupation
La(1)[a]	2e	0.224(3)	0.250	0.507(6)	0.93
La(2)[a]	2e	0.258(8)	0.250	0.003(4)	0.07
Na(1)[a]	2e	0.258(8)	0.250	0.003(4)	0.93
Na(2)[a]	2e	0.224(3)	0.250	0.507(6)	0.07
Ni	2e	0.762(1)	0.250	0.252(4)	1.00
W	2e	0.740(7)	0.250	0.729(5)	1.00
O(1)	4f	0.441(7)	0.439(6)	0.698(6)	1.00
O(2)	4f	0.024(8)	0.041(5)	0.216(5)	1.00
O(3)	2e	0.698(6)	0.250	0.528(4)	1.00
O(4)	2e	0.761(3)	0.250	0.017(9)	1.00

[a]Disordered in A-plane: 6.6%.

Table 4 Bond distances of $NaLaCoWO_6$

	d/Å		d/Å
Na–O(1)	2.328(3) × 2	La–O(1)	2.765(3) × 2
Na–O(1)	3.003(1) × 2	La–O(2)	2.419(2) × 2
Na–O(2)	2.816(1) × 2	La–O(2)	2.848(4) × 2
Na–O(3)	3.028(2)	La–O(4)	2.926(1)
Na–O(3)	2.523(1)	La–O(4)	2.621(1)
Na–O(3)	2.830(1) × 2	La–O(4)	2.776(5) × 2
d_{mean}	2.751	d_{mean}	2.717
$d_{Shannon}$	2.58	$d_{Shannon}$	2.56
W–O(1)	1.866(1) × 2	Co–O(1)	2.159(1) × 2
W–O(2)	2.102(4) × 2	Co–O(2)	1.897(4) × 2
W–O(3)	1.683(2)	Co–O(3)	2.165(1)
W–O(4)	2.214(1)	Co–O(4)	1.928(3)
d_{mean}	1.972	d_{mean}	2.034
$d_{Shannon}$	2.00	$d_{Shannon}$	2.05

Table 5 Bond distances of $NaLaNiWO_6$

	d/Å		d/Å
Na–O(1)	2.188(2) × 2	La–O(1)	2.801(1) × 2
Na–O(1)	2.993(3) × 2	La–O(2)	2.410(2) × 2
Na–O(2)	2.788(1) × 2	La–O(2)	2.831(1) × 2
Na–O(3)	2.905(1)	La–O(4)	2.748(4)
Na–O(3)	2.622(4)	La–O(4)	2.774(2)
Na–O(3)	2.806(1) × 2	La–O(4)	2.766(1) × 2
d_{mean}	2.708	d_{mean}	2.714
$d_{Shannon}$	2.58	$d_{Shannon}$	2.56
Ni–O(1)	2.085(2) × 2	W–O(1)	1.968(1) × 2
Ni–O(2)	1.872(1) × 2	W–O(2)	2.107(2) × 2
Ni–O(3)	2.198(3)	W–O(3)	1.598(1)
Ni–O(4)	1.844(1)	W–O(4)	2.270(1)
d_{mean}	1.993	d_{mean}	2.003
$d_{Shannon}$	2.09	$d_{Shannon}$	2.00

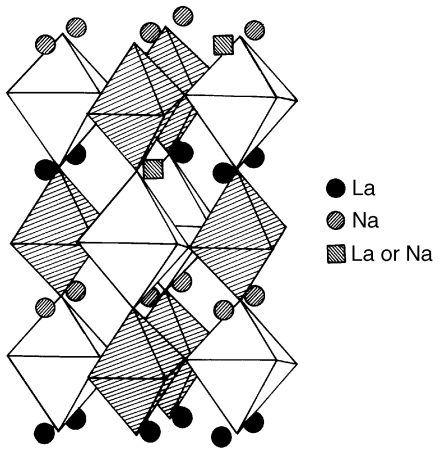

Fig. 3 Structural model for (NaLa)(NiW)O_6

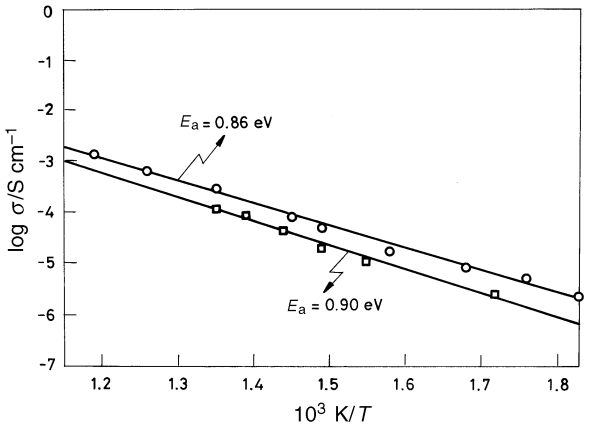

Fig. 4 log σ *vs.* reciprocal temperature for (NaLa)(MW)O_6: ○, M = Co; □, M = Ni

Physical properties

Electronic conductivity in perovskite-like materials is highly dependent on the nature of the B–O and B–O–B interactions. In the title compounds, B sites are orderly occupied by two kinds of cations, M^{2+} and W^{6+}, having different electronic configurations (d^7 Co^{2+}, d^8 Ni^{2+} and d^0 W^{6+}) and these characteristics could affect their transport properties.

Fig. 4 shows the experimental dependence of log σ *vs.* T^{-1}. The conductivity is quite low and the activation energy is relatively high in both cases suggesting that these materials are poor semiconductors. This fact could be due to the very different energies between the d orbitals of the transition metals (3d for Co and Ni and 5d for W) which interact with the oxygen p orbitals. On the other hand, there are significative distortions both in each particular BO_6 octahedron and in their tilting in the structure which are responsible for lowering the unit cell symmetry. The resulting conduction band should be mainly defined by discrete levels because of the imperfect overlap between B–O orbitals.

The magnetic susceptibility (χ) *vs.* temperature graphs for cobalt and nickel compounds are given in Fig. 5 and 6. Both materials follow a Curie–Weiss law in the temperature range 50–300 K and below 50 K a maximum appears for the cobalt derivative. Such a maximum is not detected in the nickel sample although when the product χT *vs.* T is plotted (Fig. 7) a remarkable decrease below 40 K is observed, reaching a value of 0.12 emu K mol^{-1}. Thus, the above data suggest antiferromagnetic ordering for both compounds. This kind of superexchange interaction in perovskites has been widely studied previously[11–14] and an antiferromagnetic coupling between paramagnetic cations in these materials could be produced in two possible ways: (a) between nearest-neighbour (nn) paramagnetic cations located on the same *ab* plane, that is Ni—O—O—Ni in which these oxygens form the equatorial edge of the WO_6 octahedra; (b) between next-nearest-neighbour (nnn) cations superposed along the *c* axis, involving a path defined by Ni—O—W—O—Ni in which the oxygens occupy the axial vertices of WO_6 octahedra.

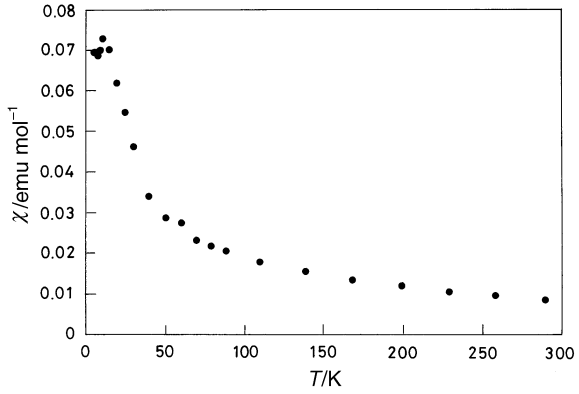

Fig. 5 Magnetic susceptibility *vs.* temperature for (NaLa)(CoW)O_6

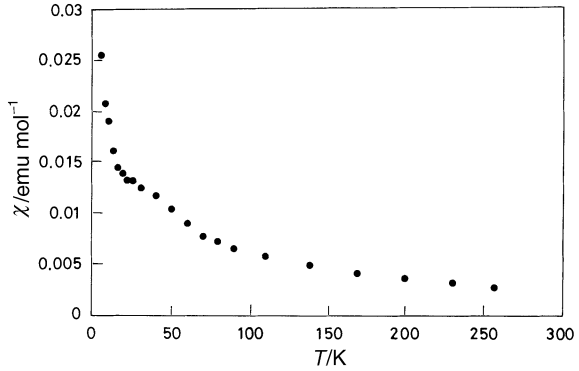

Fig. 6 Magnetic susceptibility *vs.* temperature for (NaLa)(NiW)O_6

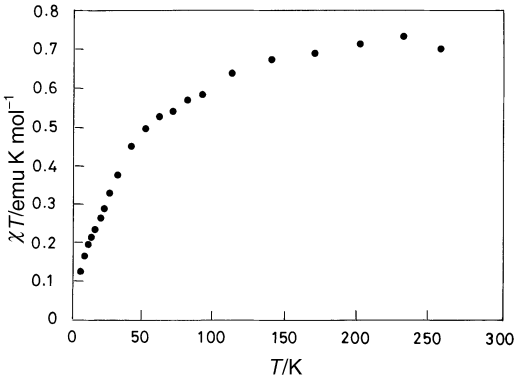

Fig. 7 χT *vs.* T for (NaLa)(NiW)O_6

In principle, path (a) seems to be the most likely to explain the antiferromagnetic properties in perovskites, although neutron diffraction data should be obtained to confirm this assumption.

Symmetry relationships in perovskites

A large number of structures related to the parent perovskite structure can be described by considering displacements of the anions (oxygen in the following discussion) or by ordering of the cations, either A or B. Simultaneously, such cations may be of different chemical nature, giving the general compositions (AA′)(BB′)O_6. At this point we shall discuss how the space group $P2_1/m$ (which was deduced for the title phases, NaLaMWO_6) is related to the cubic perovskite one, $Pm3m$. The particular examples that illustrate the different symmetry operations correspond to some perovskites previously reported by us.

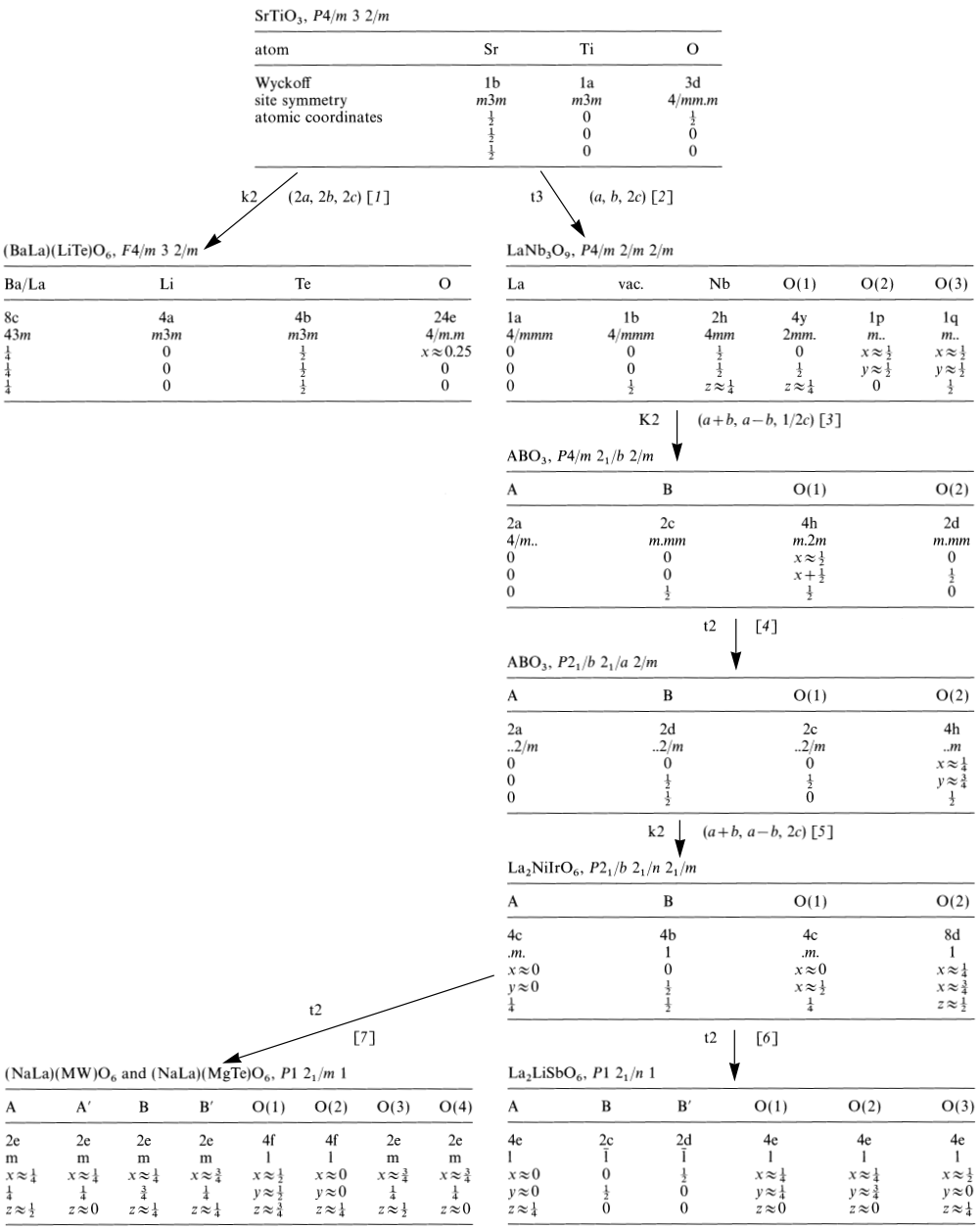

Scheme 1

Scheme 1 shows perovskite-type derivatives which are of interest in the context of ordered cation or anion displacements. Structural relations between these phases are defined by means of a group–subgroup family tree as proposed by Müller[15] and this scheme can be set up with the aid of the International Tables for Crystallography,[16] in which the maximal subgroups of every space group are listed.

Double perovskites: $AB_{0.5}B'_{0.5}O_3 \equiv A_2(BB')O_6$. When a large difference, in either charge or ionic radius, exists between two different (B and B′) cations, an ordered distribution of these cations can take place along the (111) planes, as occurs in (BaLa)(LiTe)O_6;[17] in this respect, we can consider both A cations, Ba and La, which are randomly located on the same sites, as identical from a structural point of view. The unit cell parameter (*ca.* 4 Å) in an ABO_3 simple perovskite requires enlargement when B and B′ cations are ordered in the structure and the new space group is a *Klassengleiche* subgroup in which the symmetry reduction is of index 2 (**k2**) belonging to the same crystal class. The reduction in symmetry takes place by the loss of translation operations, either by enlargement of the unit cell or by showing up a new centreing. Since the space group symbol itself states only symmetry operations, it gives no information about the atomic positions that are occupied in each particular structure, and additional data concerning these positions are necessary for every member of the family tree (atom coordinates, site symmetries and number of equivalent positions).

Family tree [1] in Scheme 1 shows the essential data for transforming $SrTiO_3$ into the new structure of (BaLa)(LiTe)O_6 and the relation between them is depicted in Fig. 8 (*ab* plane). From this relation the necessity of doubling the unit cell parameter with respect to $SrTiO_3$ clearly arises and the symmetry reduction that takes place imposes eight formulae per unit cell.

Perovskite with double *c*-axis: $La_{1/3}NbO_3 \equiv LaNb_3O_9$. Other different changes in symmetry appear when there are changes in the A sublattice. For example, $La_{1/3}NbO_3$[18] is a well known cation-deficient perovskite where half of the A planes are vacant and in the remaining ones only two-thirds of such sites are occupied in an alternating sequence. This arrangement implies a doubled *c* axis and the symmetry reduction in this case is accomplished by the disappearance of the three-fold axes and the maximal non-isomorphic subgroup is *Translationengleiche* of index 3 (t3). Family tree [2] shows the

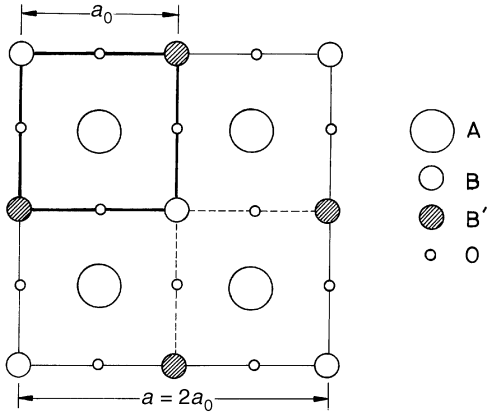

Fig. 8 Relationship between ABO_3 and $A_2BB'O_6$ perovskites

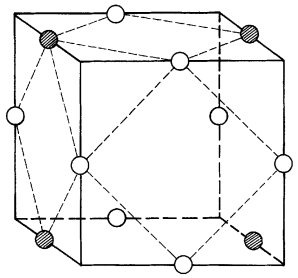

Fig. 9 A-cation coordination polyhedra in perovskite showing the reduction from twelve- to eight-coordination (by loss of the four shaded circles)

group–subgroup relationship between $SrTiO_3$ and $LaNb_3O_9$ as well as the atomic coordinates and Wyckoff site.

Oxygen displacement in perovskites. In the previous examples the A cations possess a cuboctahedral coordination which is compatible with the relative size of the remaining ions implied in such structures. A reduction in the A polyhedra takes place when the A cations are relatively smaller; for instance, in La_2NiIrO_6[19] lanthanum is eight-coordinate. These new polyhedra are defined as distorted bicapped prisms which can be related to the cuboctahedral ones by the loss from the latter of four oxygen anions located on four opposite edges in the unit cell. Fig. 9 shows an idealized view of this transformation. There is a movement of oxygen anions that produces a tilting of BO_6 octahedra on the [001] and [110] directions of the parent structure.[20] The space group of La_2NiIrO_6 is *Pbnm* but it is not a subgroup of *P*4/*mmm* and therefore the changes are somewhat complicated and several steps are necessary to achieve the complete transformation.

The first step (family tree [3]) involves the change of *P*4/*mmm* into *P*4/*mbm*, having in mind that the second is a k2 subgroup of the first, and the symmetry reduction takes place by enlargement of the old unit cell. The new parameters are related to the cubic one, a_o, as follows: $a=b\approx a_o\sqrt{2}$ and $c\approx a_o$. Fig. 10 shows the oxygen displacements, which only affect atoms located on equatorial positions (*ab* plane) of BO_6 octahedra. The disappearance of the two-fold axes parallel to *x* or *y* and of the *m* plane normal to them, which are transformed into translation symmetry elements of the same nature, takes place. Such BO_6 octahedra undergo severe distortions (Fig. 10, left) and the oxygen atoms labelled 1–4, displaced along the *x* and *y* axes, are related by a four-fold axis located in the centre of the graph (Fig. 10, right). The full symbol for the new space group would be $P4/m2_1/b2/m$.

A further transformation t2 allows the formation of the maximal non-isomorphic subgroup *Pbam*, orthorhombic, as is depicted in Fig. 11. The symmetry reduction in this case is accomplished by the substitution of the four-fold axis by a two-fold screw 2_1 axis and also involves the loss of the two-fold axis and the *m* plane parallel and normal to (110) planes, respectively. The remaining symmetry elements become clear in the full symbol of the new space group: $P2_1/b2_1/a2/m$. Family tree [4] in Scheme 1 shows the above transformation.

The last step for giving the complete description of the A coordination polyhedra is the relation between the last space group and *Pbmn* (corresponding to the phase La_2NiIrO_6) shown in Fig. 12. Apical oxygens of BO_6 octahedra (located on the [001] direction in the parent structure) are displaced in zigzags, doubling the *c*-axis ($c=2a_o$) and provoking the concomitant symmetry reduction. The actual space group is a non-isomorphic k2. On the other hand, A cations are also moved from their ideal sites to occupy the centres of the new distorted polyhedra (see for instance the positions of the A

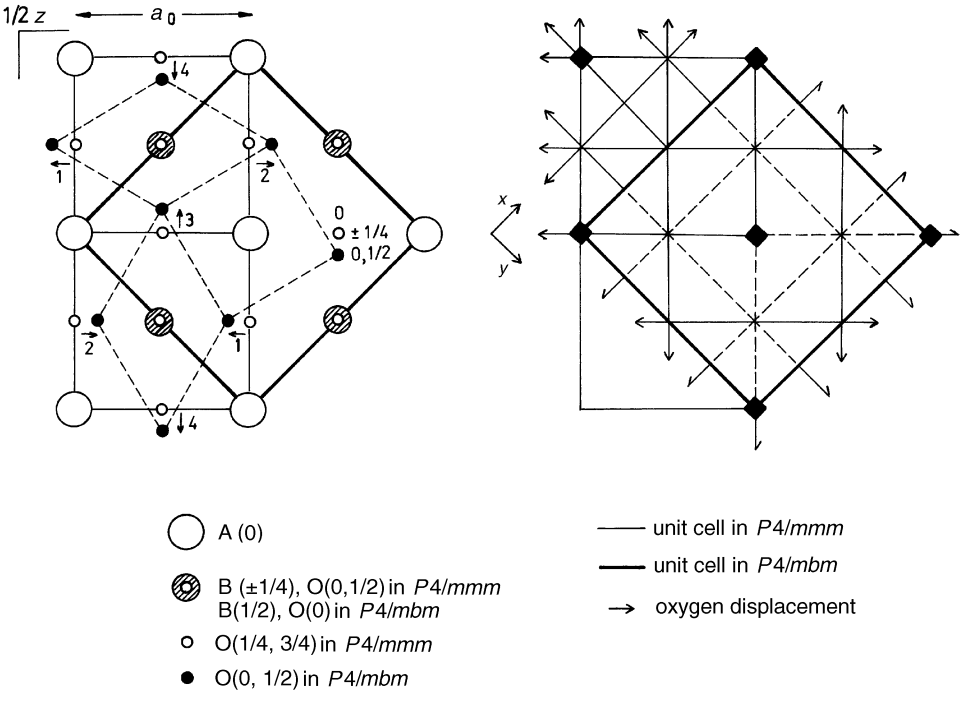

Fig. 10 Structural and symmetry relationships between *P*4/*mmm* and *P*4/*mbm*

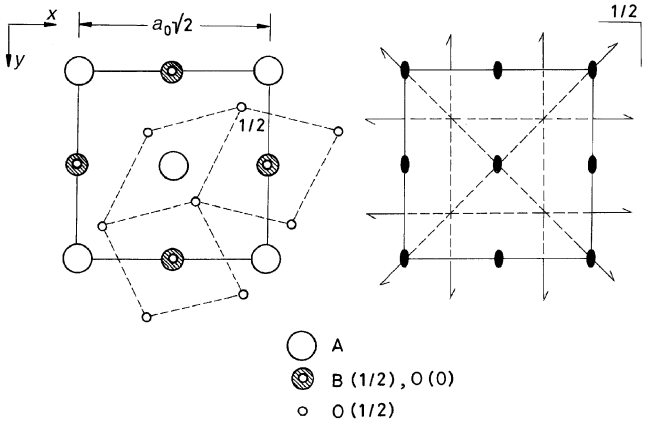

Fig. 11 Structural and symmetry relationships between *P*4/*mbm* and *Pbam*

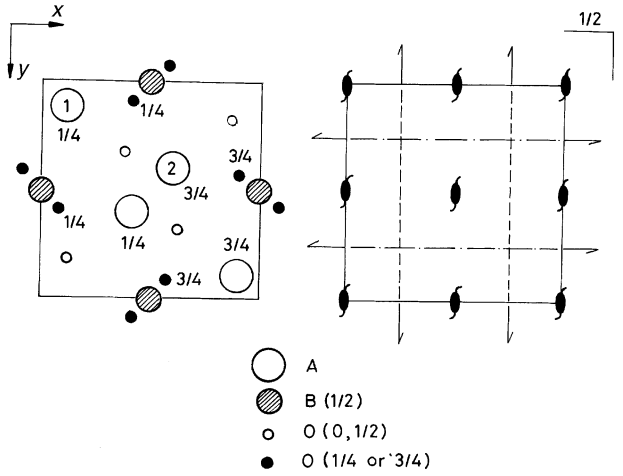

Fig. 12 Structural and symmetry relationships between *Pbam* and *Pbmn*

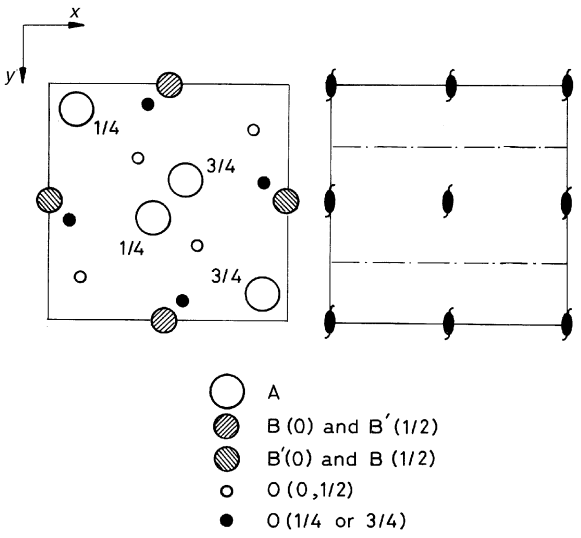

Fig. 13 Structural and symmetry relationships between *Pbmn* and $P2_1/n$

atoms, labelled as 1 and 2, in Fig. 12). The structural arrangement gives rise to the conversion of *a* planes (normal to the *y* axis) into *n* glide planes and the simultaneous transformation of the former two-fold rotation axes into two-fold screw axes (full notation of the space group: $P2_1/b2_1/n2_1/m$). Family tree [5] summarizes these transformations.

Let us consider now two particular cases derived from this latter structure. The first example is referred to as La_2LiSbO_6,[21] in which La^{3+} cations are placed on eight-coordinate sites,

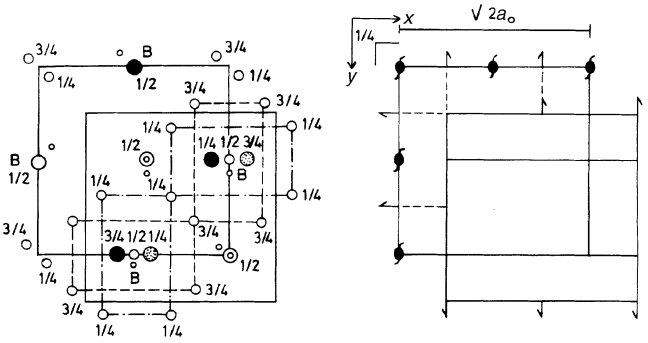

Fig. 14 Structural and symmetry relationships between *Pbmn* and $P2_1/m$

and where the high charge difference between Li^+ and Sb^{5+} formal cations provokes the ordering of the LiO_6 and SbO_6 octahedra in the structure, by sharing corners (Fig. 13). The new group, $P2_1/n$ belonging to the monoclinic crystal system (although β is always close to 90°), results from the symmetry reduction by removal two mutually perpendicular two-fold axes, along *x* and *y*, as well as their respective normal glide planes. All these changes result from a t2 subgroup as is indicated by tree [6].

Finally, when there are two kinds of different cations with a large difference in charge in the A sublattice, an ordered arrangement in the *ab* plane is found; for instance, in the two phases reported in this work and also in a related compound previously described by us, (NaLa)(MgTe)O_6.[7] The final space group is $P2_1/m$ and is again the result of a t2. One can deduce from Fig. 14 that a change of origin must occur. This change, the atom sites and the Wyckoff site symmetry are shown in tree [7].

Financial support from CICYT is acknowledged (MAT94-079).

References

1 A. F. Wells, *Structural Inorganic Chemistry*, Clarendon, Oxford, 5th edn., 1984.
2 A. R. West, *Solid State Chemistry*, Wiley, New York, 1990.
3 B. G. Hyde and S. Anderson, *Inorganic Crystal Structures*, Wiley, New York, 1989.
4 A. M. Glazer, *Acta Crystallogr., Sect. B*, 1972, **28**, 3384.
5 M. T. Anderson, K. B. Greenwood, G. A. Taylor and K. R. Poeppelmeier, *Prog. Solid State Chem.*, 1993, **22**, 197.
6 T. Sekiya, T. Yamamoro and Y. Torii, *Bull. Chem. Soc. Jpn.*, 1984, **57**, 1859.
7 M. L. Lopez, M. L. Veiga and C. Pico, *J. Mater. Chem.*, 1994, **4**, 547.
8 H. M. Rietveld, *J. Appl. Crystallogr.*, 1969, **2**, 65.
9 J. Rodríguez-Carvajal, Program Fullprof, ILL, Grenoble, France, 1994, unpublished work.
10 *Theory and Applications of Molecular Paramagnetism*, ed. L. N. Mulay and E. A. Boudreaux, Wiley, New York, 1976, p. 494.
11 M. P. Attfield, P. D. Battle, S. K. Bollen, S. M. Kim, D. V. Powell and M. Workman, *J. Solid State Chem.*, 1992, **96**, 344.
12 P. D. Battle and W. J. Macklin, *J. Solid State Chem.*, 1993, **52**, 138.
13 P. D. Battle and W. J. Macklin, *J. Solid State Chem.*, 1984, **54**, 245.
14 P. D. Battle, T. C. Gibb and C. W. Jones, *J. Solid State Chem.*, 1989, **78**, 281.
15 U. Müller, *Inorganic Structural Chemistry*, Wiley, New York, 1993.
16 *International Tables for Crystallography*, Theo Hahn, Boston, 1987, vol. A, 2nd edn.
17 M. L. López, A. Jerez, C. Pico, R. Saéz-Puche and M. L. Veiga, *J. Solid State Chem.*, 1993, **105**, 19.
18 P. Yyer and A. I. Smith, *Acta Crystallogr.*, 1967, **23**, 740.
19 E. M. Ramos, I. Alvarez, M. L. Veiga and C. Pico, *Mater. Res. Bull.*, 1994, **29**, 861.
20 W. A. Groen, F. P. F. Van Berkel and D. I. W. Ijdo, *Acta Crystallogr., Sect. C*, 1986, **42**, 1472.
21 M. Lopez, M. L. Veiga, J. Rodriguez, F. Fernandez, A. Pico and C. Pico, *Mater. Res. Bull.*, 1992, **27**, 647.

Paper 6/05206A; *Received* 25*th July*, 1996